EXPERIMENTS ON THE COMPARISON BETWEEN CASCADE AND AXIAL-FLOW COMPRESSOR PERFORMANCES

PART II: EXPERIMENT ON AXIAL-FLOW COMPRESSOR*

SHINTARO OTSUKA

Department of Aeronautical Engineering

and TADASHI HIKI**

(Received July 10. 1962)

Introduction

As was explained in the part I of this series of papers[1], this experiment was performed for the purpose of the most simple comparison between cascade and axial-flow compressor performances. The following matters were especially kept in mind throughout this experiment: apparatuses were made carefully to keep measurement error minimum, and measuring instruments which were believed to be as small as possible and to indicate the most reliable data were adopted. This report does not cover the comparison between cascade and axial-flow compressor, which will be accomplished in the sequel.

Symbols

a: blade pitch
c: chord length
C_d: loss coefficient $\quad C_d=\dfrac{(p_{s1}+\frac{1}{2}\rho V_1^2)-(p_{s2}+\frac{1}{2}\rho V_2^2)}{\frac{1}{2}\rho V_1^2}$
p: pressure
r: radial position of blade element
u: peripheral velocity $\quad u=r\omega$
V: velocity relative to moving blade
w: absolute velocity
α: stagger angle
α_i: attack angle
β: turning angle
Γ: blade circulation
γ: angle between velocity relative to moving blade and its cascade axis
Δp: pressure rise $\quad \Delta p=p_2-p_1$
θ_a: angle between absolute velocity and compressor axis
ρ: density

* The 20th Report of the Study on Axial-flow Turbo-machines.
** Engine Division, Transportation Technical Research Institute.

φ: flow coefficient $\varphi = \frac{w_a}{r\omega}$, $\left(\varphi_i = \frac{w_a}{r_i\omega}\right)$

ψ: pressure coefficient $\psi = \frac{\Delta p_T}{\frac{1}{2}\rho(r\omega)^2}$, $\left(\psi_i = \frac{\Delta p_T}{\frac{1}{2}\rho(r_i\omega)^2}\right)$

ω: angular velocity

Subscript:

1: before rotor
2: behind rotor
a: axial
i: inner (hub) wall, (see α_i)
o: outer (casing) wall
S: static
T: total
t: tangential

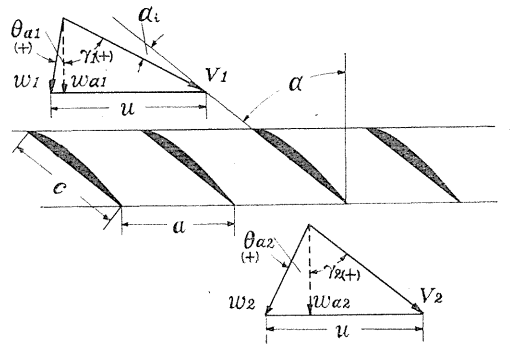

FIG. 1

Apparatus and Procedure

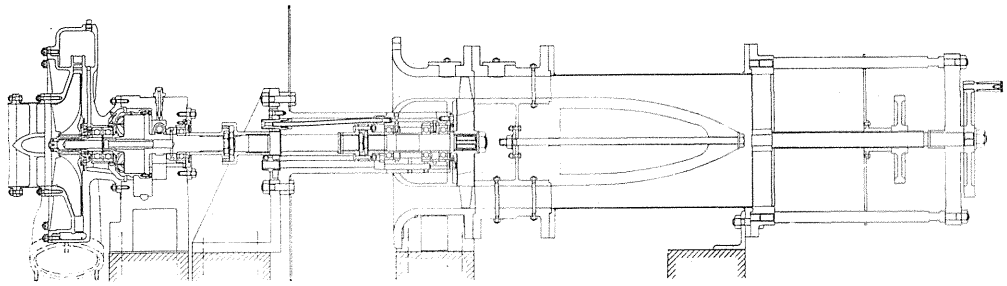

FIG. 2

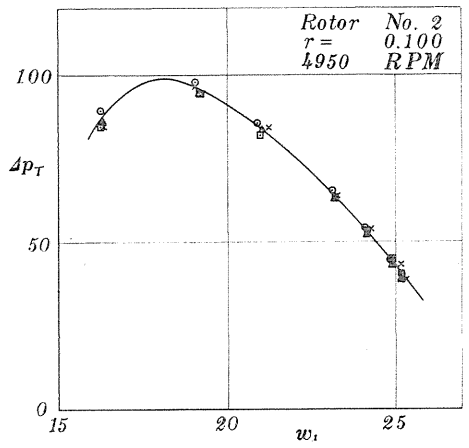

FIG. 3

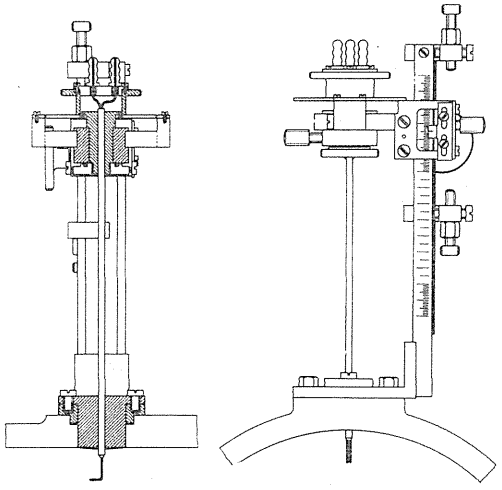

FIG. 4

The axial-flow compressor used is illustrated in the schematic drawing of Fig. 2. This equipment was prepared especially for this experiment. The power is supplied by the air-turbine illustrated in the left end of the drawing. The air-turbine was reconstructed from the super-charger of Daimler Benz DB-600 engine. The air is supplied from the separate air source. The axial-flow compressor has moving blades but no stationary blade. The latter can be attached if it is required in the future experiment. A special design feature is that there is no obstacle such as strut in the upstream of moving blades. Therefore it is believed that the most reliable data can be obtained. Casing internal diameter is 240 mm, and hub diameter is 160 mm. The latter can be reduced to 110 mm by changing hub fittings.

Air speed and yaw measurements were done at different peripheral positions. This is because large probes are needed for the measurements at the same po-

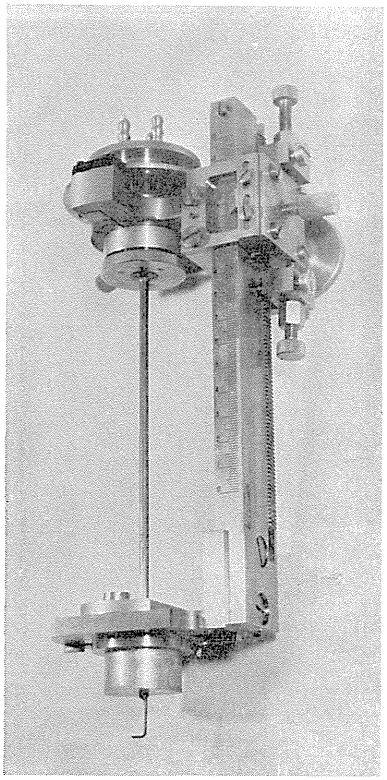

FIG. 5(a)

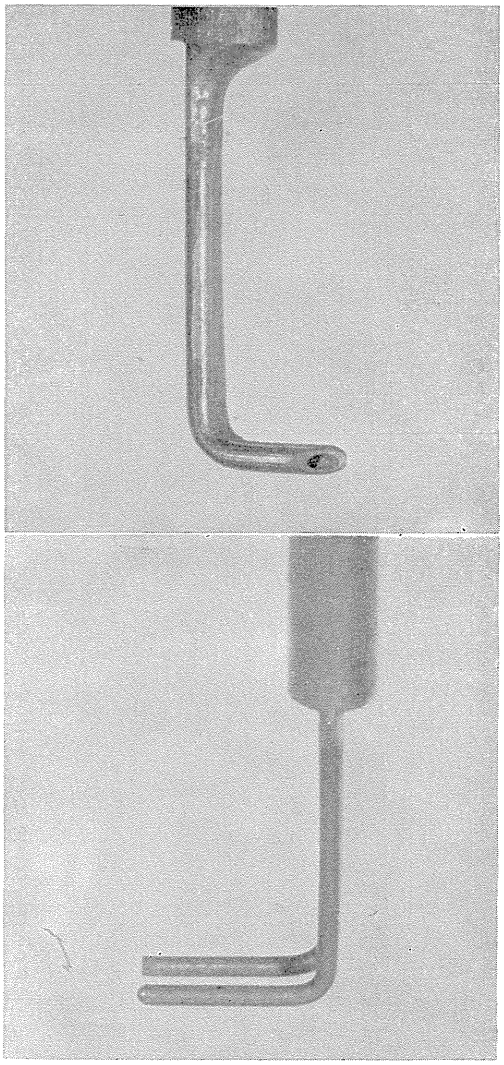

FIG. 5(b)

sition, and measurement error increases. The peripheral uniformness of flow was sufficiently checked. An example is illustrated in Fig. 3. Fig. 4 is the drawings of traversing device, and Fig. 5 is photographs of it, pitot tube and yaw probe. Pitot tubes and yaw probes were made with copper tube of 1 mm in diameter.

TABLE 1.

Rotor No.	r	α	a/c
1	0.119	77.13°	1.70
	0.110	75.25	1.44
	0.101	73.32	1.22
	0.092	71.50	1.03
	0.083	69.65	0.87
2	0.119	67.40°	1.70
	0.110	64.90	1.44
	0.101	62.22	1.22
	0.092	59.02	1.03
	0.083	55.57	0.87
3	0.119	50.20°	1.70
	0.110	46.33	1.44
	0.101	42.75	1.22
	0.092	39.52	1.03
	0.083	36.45	0.87
Casing Radius			0.120
Hub Radius			0.080
Tip Clearance			0.0005

RAF-6

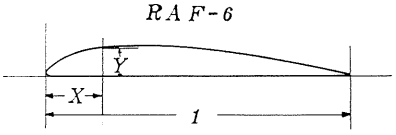

X	Y
0.025	0.041
0.050	0.059
0.100	0.079
0.200	0.095
0.300	0.100
0.400	0.099
0.500	0.095
0.600	0.087
0.700	0.074
0.800	0.056
0.900	0.035
leading edge radius	0.010
trailing edge radius	0.0077

FIG. 6

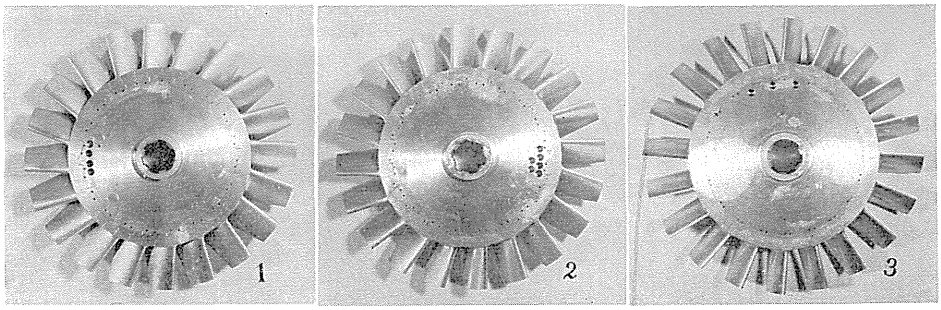

FIG. 7

Three rotors with blades of different setting angles were made. No. 1 has the largest stagger angle, and No. 3 has the smallest. Free vortex blades were aimed in the design, but because of the error in manufacture twist angles are pretty different from the values designed. Nevertheless, blade profile dimension has the error of only within 0.02 mm and is very good. Table 1 indicates the results of actual measurement in which α is the mean value of 20 blades. The scatters of values are within 1°. Blade numbers are 20 on each rotor as above mentioned and blade profile is RAF-6 of 10% thickness. (Fig. 6) Chord length

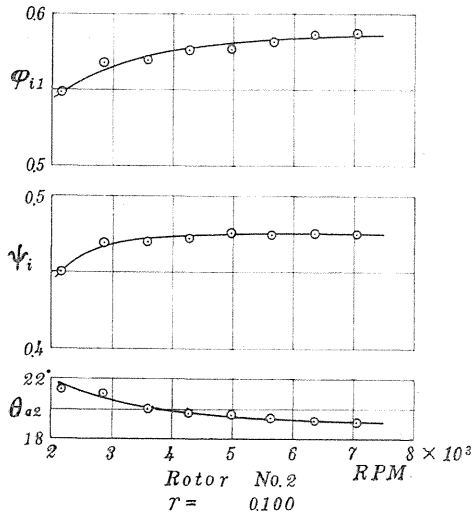

FIG. 8

is 22 mm at r=0.119 and 30 mm at r=0.083, and straight taper is used. Fig. 7 is the photographs of rotors.

Reynolds number effect was checked by varying the rotational speed, and an example is illustrated in Fig. 8. Considering the data obtained by cascade experiment[1], rotational speeds of rotor 1, 2 and 3 were determined respectively to 7140, 5712 and 4284 rpm. The number of revolution mentioned above was controlled in the experiments by a stroboscope driven by the tuning fork, therefore its accuracy is very high.

Results and Considerations

Fig. 9 is characteristic curves measured at the mid-position of blade height (r=0.100) of three rotors. Fig. 10 (a), (b) and (c) illustrate axial speed distributions in response to flow quantity changing. Fig. 11 is also flow angles behind rotor. Flow angles before rotor are almost always very near to zero.

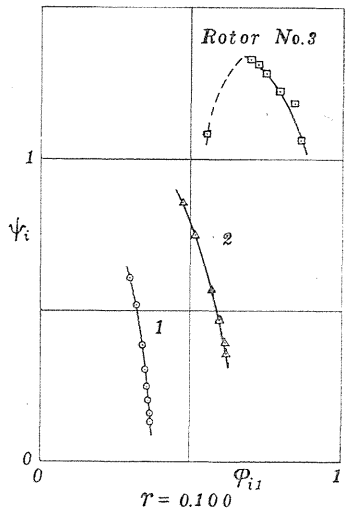

FIG. 9

The above curves are raw results obtained from the experiments. Adjusting these results we got the following values of blade elements, that is turning angle β, circulation Γ, axial velocity ratio w_{a2}/w_{a1} and loss coefficient C_d, which are illustrated in and after Fig. 12.

Values of β and Γ indicate a little scatter but its grade is likely as that we can draw curves through them. Values of w_{a2}/w_{a1} show considerable scatter and their tendencies are also divergent. Though the cause of these results is not clear, the authors suppose that it arises from complex phenomena accompained by secondary flows.

Cases a/c=1.67 (r=0.118) and a/c=0.83 (r=0.081) are included in the boundary layers, but curves of β and Γ indicate no remarkable feature. C_d is a little larger

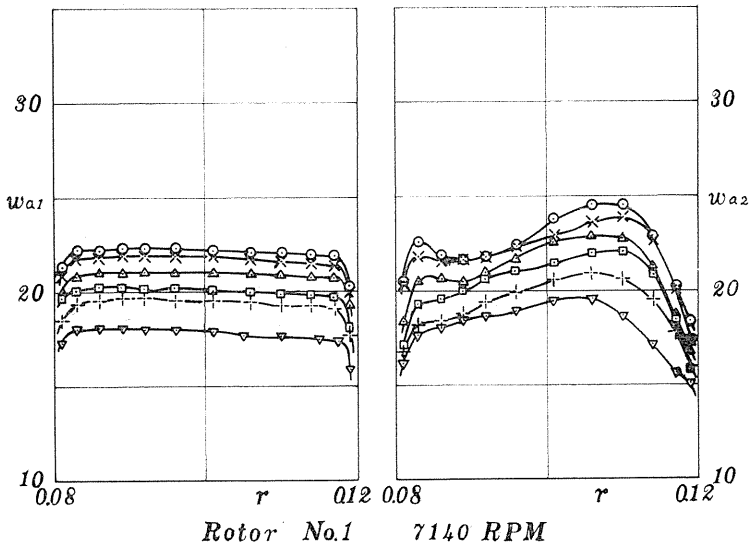

FIG. 10 (a)

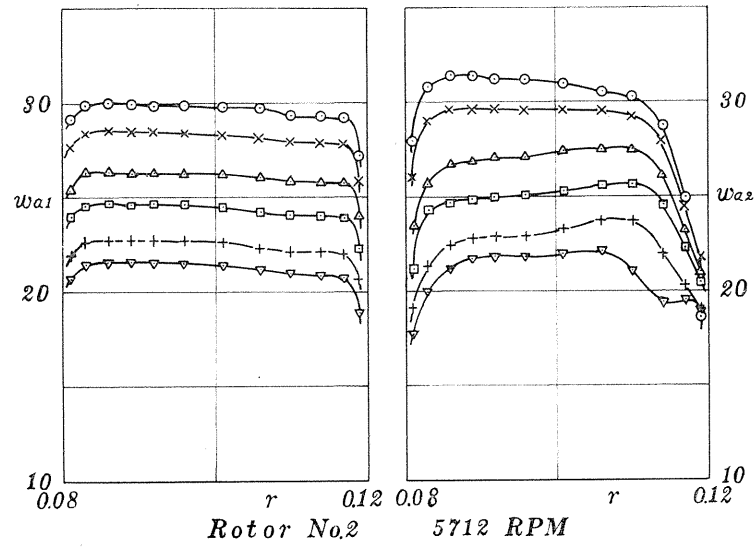

FIG. 10 (b)

and w_{a2}/w_{a1} is less than 1, these are only features attracting attention. Generally speaking, values of w_{a2}/w_{a1} are much nearer to 1 than cascade experiments. The authors suppose that this is the cause of the performance (efficiency) of axial-flow compressor to be fairly good and the cause that the cascade data cannot be applied directly to the axial-flow compressor.

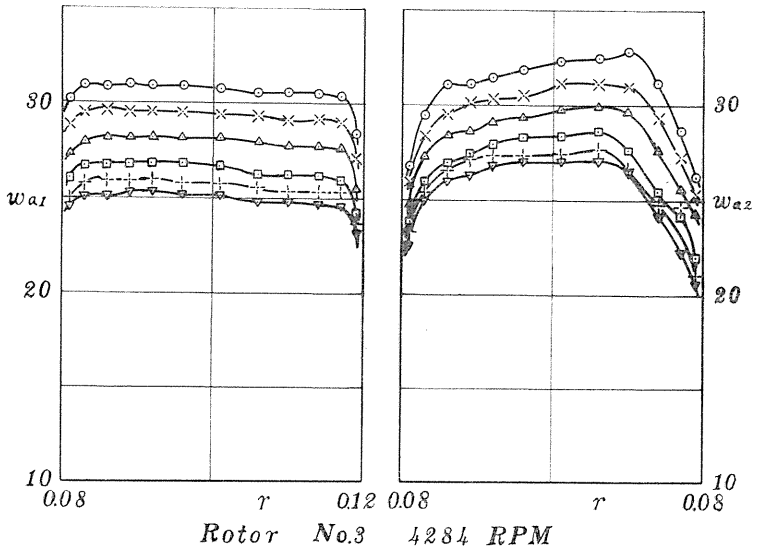

FIG. 10 (c)

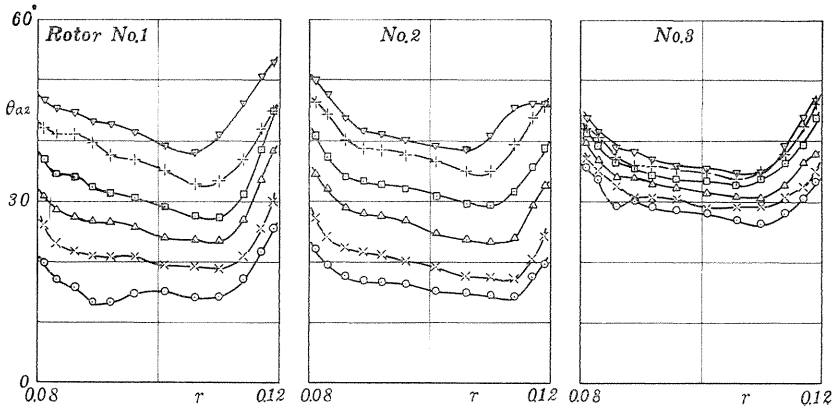

FIG. 11

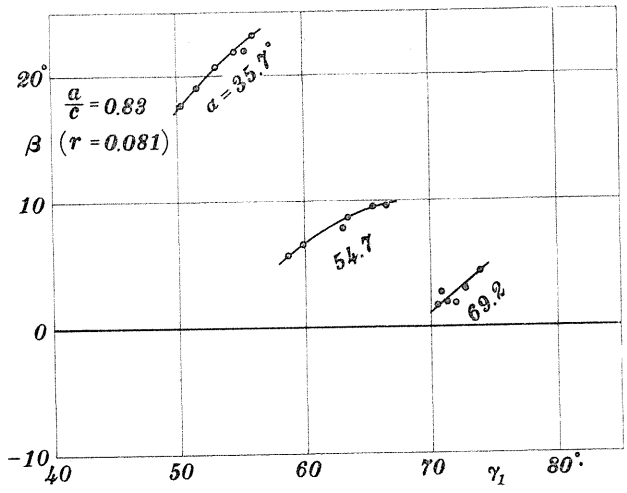

FIG. 12 (a)

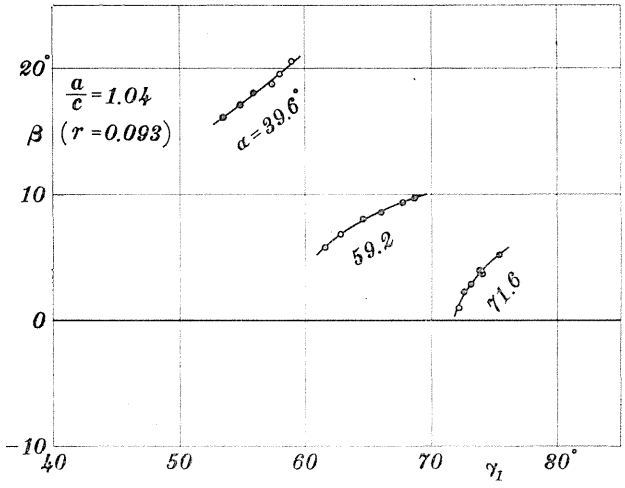

FIG. 12 (b)

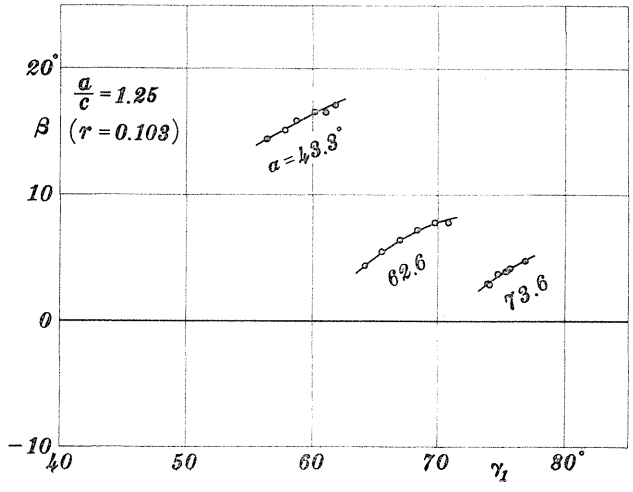

FIG. 12 (c)

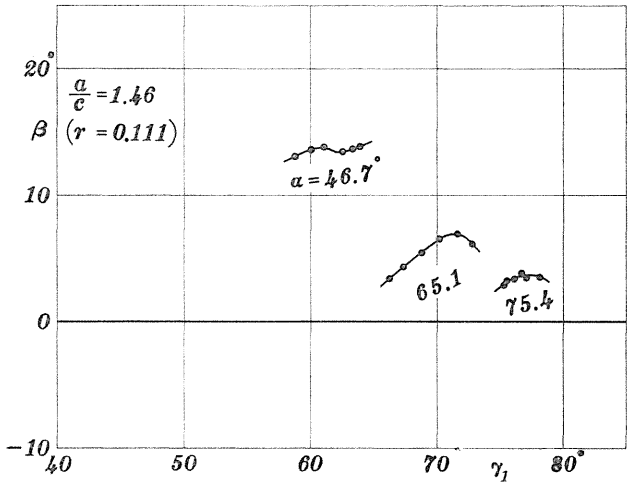

FIG. 12 (d)

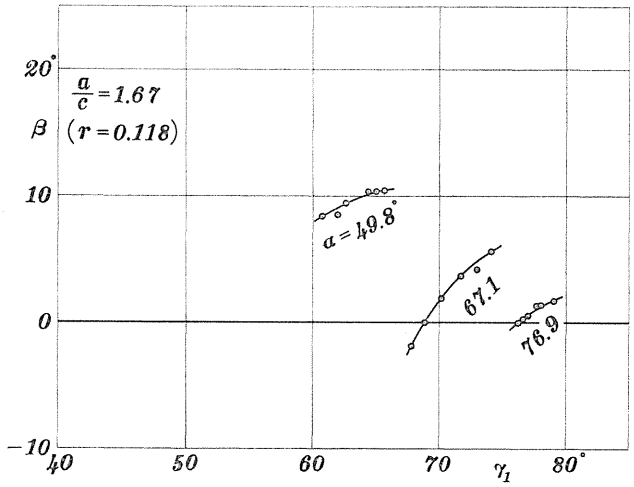

FIG. 12 (e)

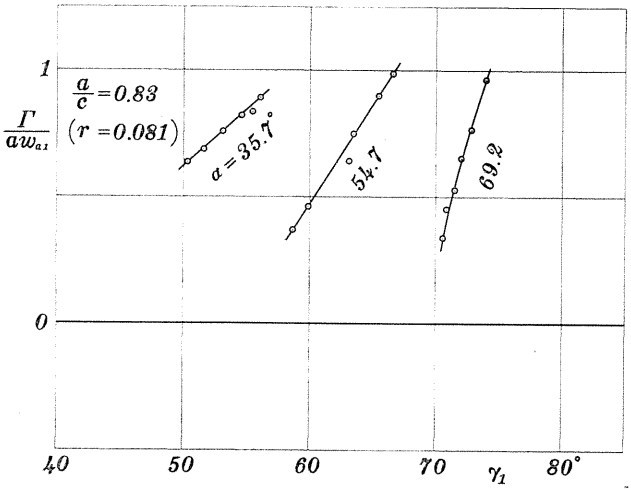

FIG. 13 (a)

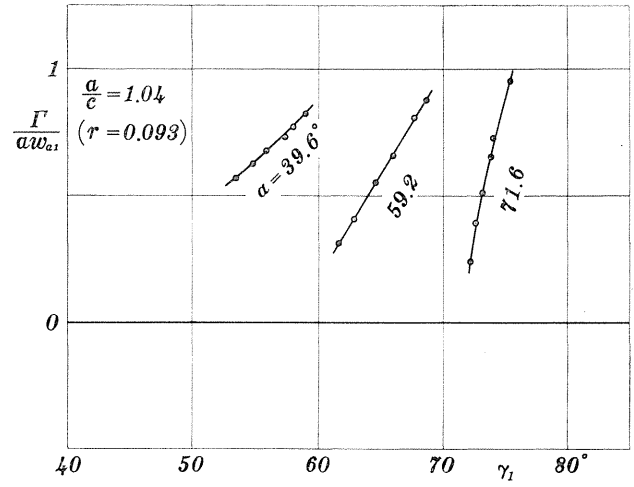

FIG. 13 (b)

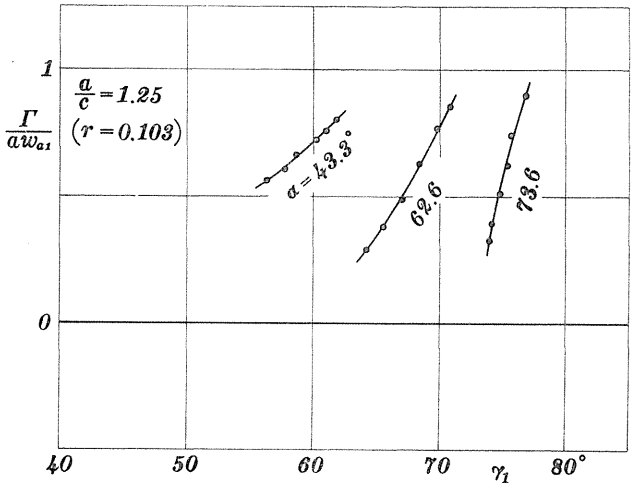

FIG. 13 (c)

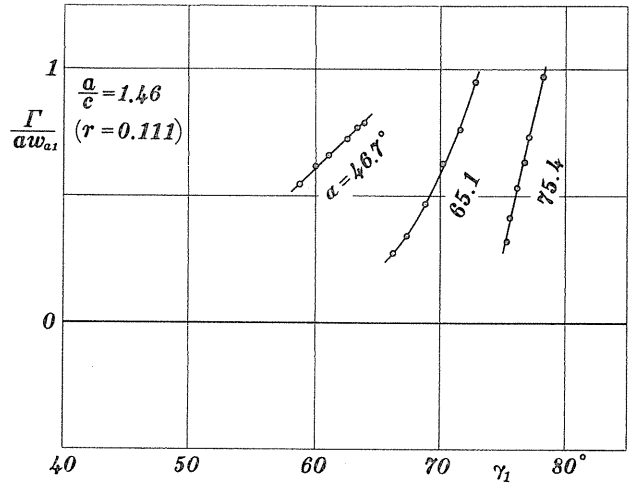

FIG. 13 (d)

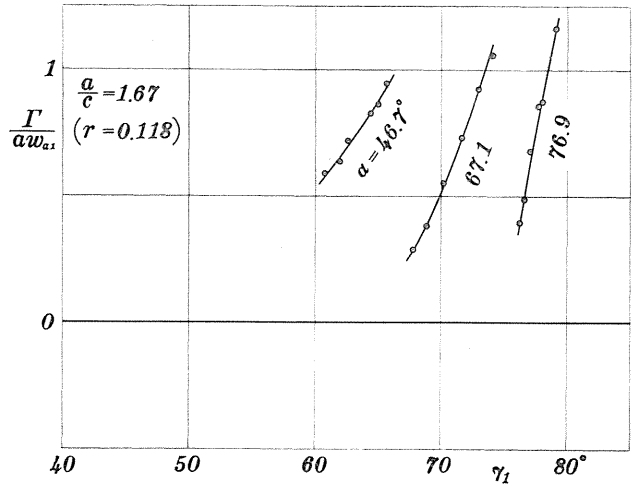

FIG. 13 (e)

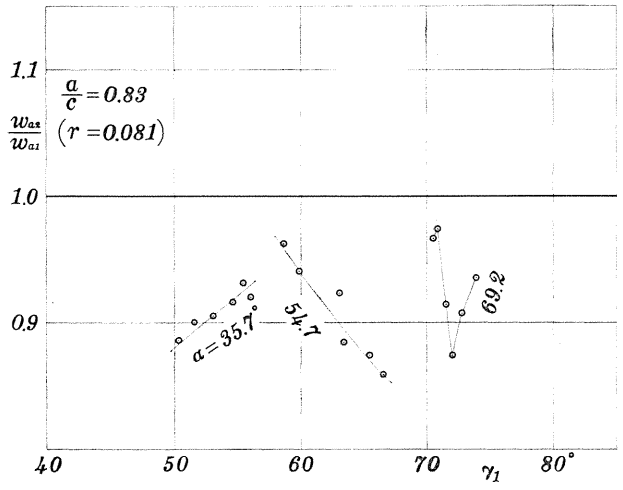

FIG. 14 (a)

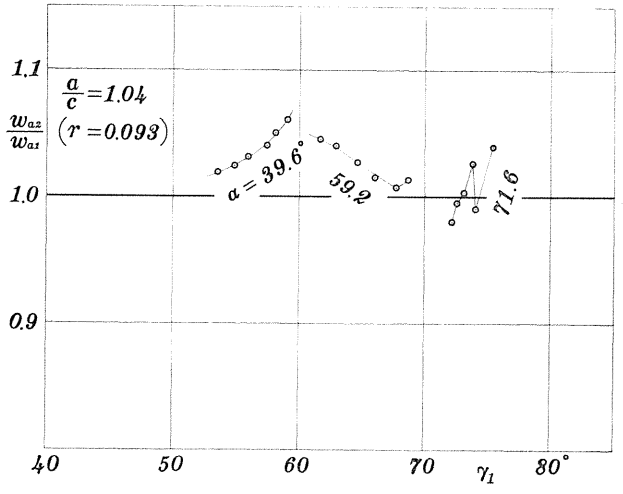

FIG. 14 (b)

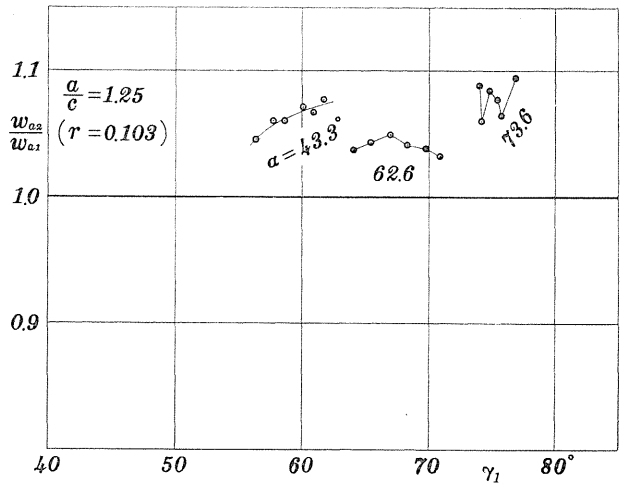

FIG. 14 (c)

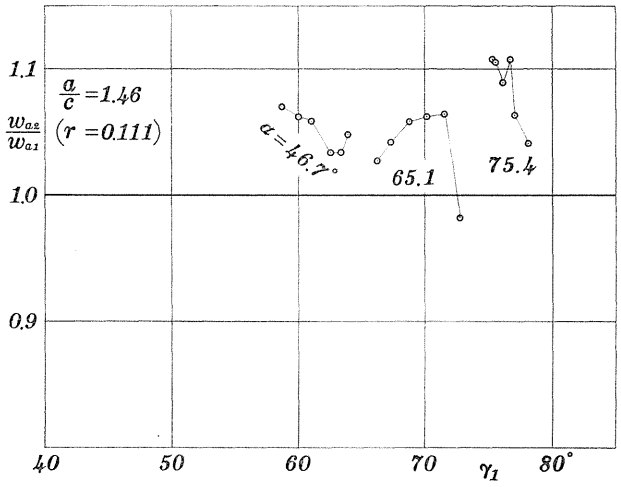

FIG. 14 (d)

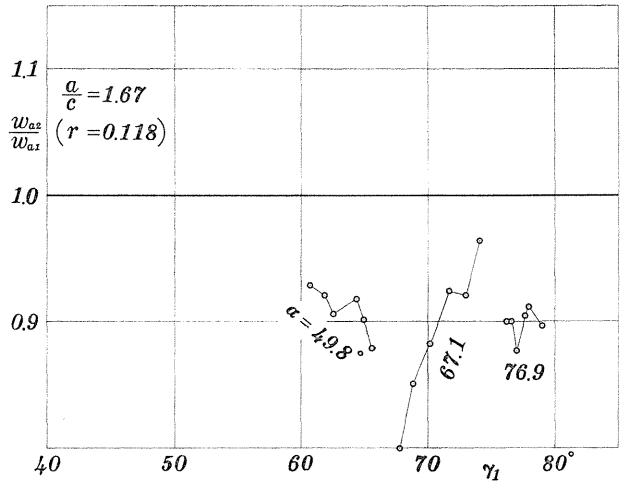

FIG. 14 (e)

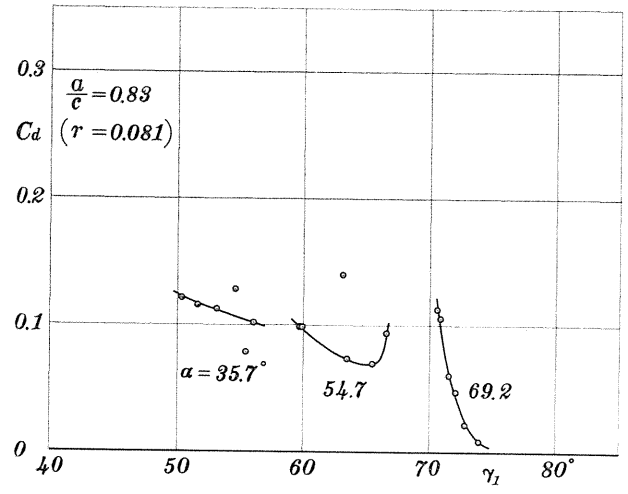

FIG. 15 (a)

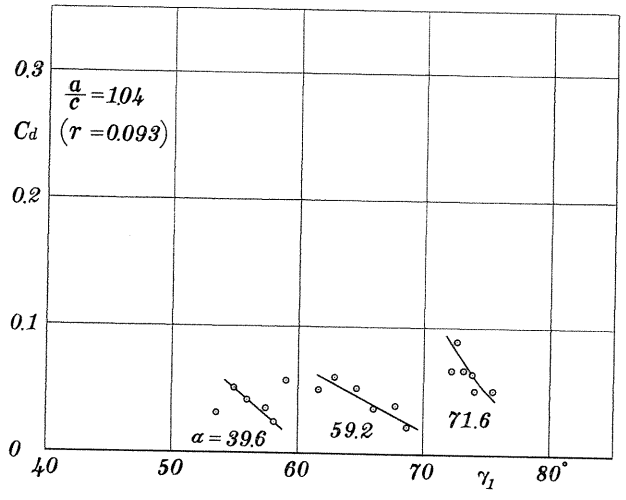

FIG. 15 (b)

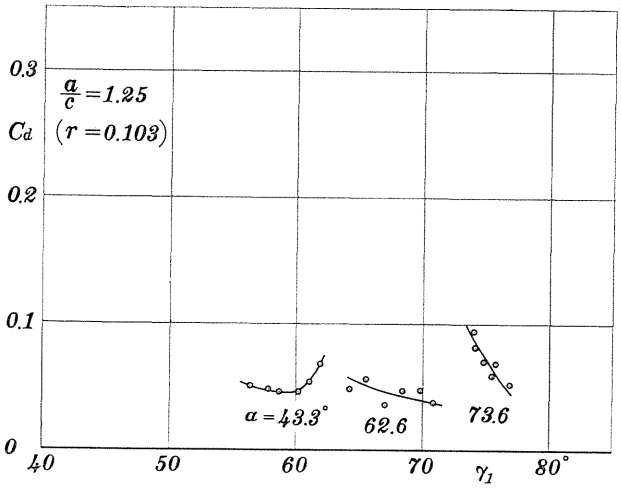

FIG. 15 (c)

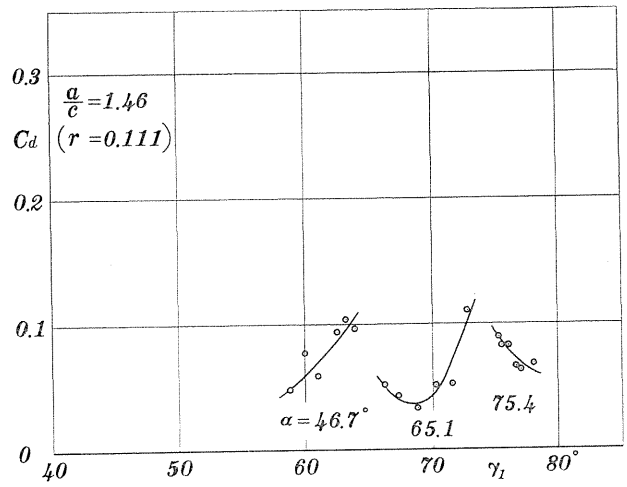

FIG. 15 (d)

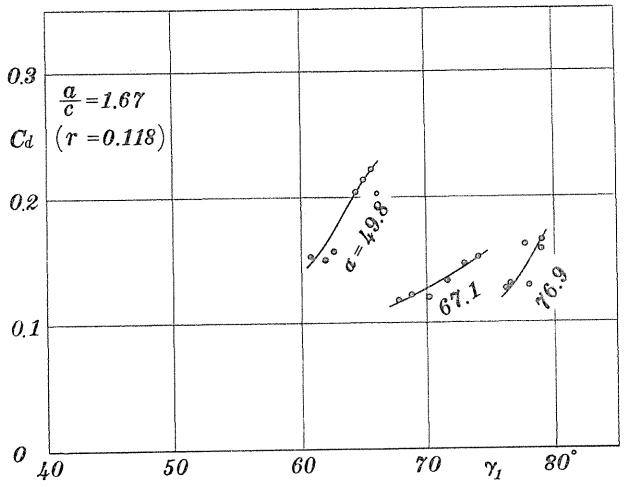

FIG. 15 (e)

References

1) Otsuka and Sato: Experiments on the Comparison between Cascade and Axial-flow Compressor Performances (part I: Experiment on Cascades), Memoirs of the Faculty of Engineering, Nagoya Univ. Vol. 14 No. 1 1962.